



## OPEN Photoperiod effects on corticosterone and seasonal clocks in cafeteria-induced obese fischer 344 rats are influenced by gut microbiota

Verónica Arreaza-Gil<sup>1,2,3</sup>, Iván Escobar-Martínez<sup>1</sup>, Jorge R. Soliz-Rueda<sup>1,2,3</sup>, Manuel Suárez<sup>1</sup>, Begoña Muguerza<sup>1</sup>, Harriet Schellekens<sup>2,3</sup>✉, Cristina Torres-Fuentes<sup>1</sup>✉ & Anna Arola-Arnal<sup>1</sup>

Seasonal rhythms are gaining attention given their impact on metabolic disorders development such as obesity gut microbiota is emerging as a key factor in mediating this link. However, the underlying mechanisms are still poorly understood. In this regard, corticosterone may play a role as it has been shown to be affected by gut bacteria and seasonal rhythms, and has been linked to obesity. Thus, this study aimed to investigate if seasonal rhythms effects on corticosterone are influenced by gut microbiota in obese rats and whether this may be related to seasonal and clock genes expression in the pituitary gland and colon. Fischer 344 male rats fed with cafeteria diet (CAF) were housed under different photoperiods for 9 weeks and treated with an antibiotic cocktail (ABX) in drinking water during the last 4 weeks. Rats fed with standard chow and CAF-fed rats without ABX were included as controls. ABX altered gut microbiota, corticosterone levels and seasonal clock expression in the pituitary depending on photoperiod conditions. These results suggest a link between gut bacteria, seasonal rhythms and corticosterone and a novel nutrigenomic target for obesity.

**Keywords** *Eya3*, *Chga*, Antibiotic, Seasonal rhythms, Western diet

Obesity and metabolic-related disorders are one of today's major health problems, with an increasing prevalence in most countries<sup>1</sup>, and strongly related to modern lifestyle factors, such as consumption of hypercaloric diets<sup>2</sup>, variations in eating patterns<sup>3</sup> or alterations in natural light/dark cycles<sup>4</sup>. These factors can directly alter the synchronization and normal function of biological rhythms (seasonal and circadian)<sup>5</sup>, which play a crucial role in maintaining host homeostasis<sup>6</sup>, promoting misalignments linked to metabolic disorders<sup>7</sup>. Therefore, studying how biological rhythms influence the development of obesity is of great interest and could lead to new treatment approaches.

Seasonal rhythms, which are characterized by differences in day length (photoperiod), emerge as key factors modulating several physiological and metabolic processes such as neuroendocrine response, metabolism, adipose tissue regulation and reproductive activity depending on the time of year<sup>8,9</sup>. These seasonal changes are modulated by the seasonal clock, which is located in the pituitary gland (also known as hypophysis), and in particular in the melatonin-responsive thyrotroph cells (calendar cells)<sup>10,11</sup>. These calendar cells operate as a binary switch mechanism, regulating the transcription of both the co-activator eyes-absent-3 (*Eya3*) and the chromogranin-A (*Chga*) in a photoperiod-dependent manner, initiating a cascade of molecular events in the pituitary gland that translates into seasonal changes in neuroendocrine function in the hypothalamus<sup>12</sup>. Moreover, these variations in day length among seasons are the external driver of the central pacemaker of circadian rhythms<sup>13–15</sup>. Hence, circadian clock genes daily profiles have been reported to be affected by photoperiod conditions<sup>16</sup>. This fact is important as circadian rhythms, which have been extensively studied, play a crucial role in regulating physiological and metabolic activities in the organism on a 24 h timescale<sup>7</sup>. Thus, circadian rhythms are driven by clock genes located both in the suprachiasmatic nucleus (SCN) (central clock) and peripheral tissues (peripheral clocks)<sup>17</sup>, consisting of an autoregulatory transcription-translation

<sup>1</sup>Nutrigenomics Research Group, Departament de Bioquímica i Biotecnologia, Universitat Rovira i Virgili, 43007 Tarragona, Spain. <sup>2</sup>Department of Anatomy and Neuroscience, University College Cork, Cork, Ireland. <sup>3</sup>APC Microbiome Ireland, Cork, Ireland. ✉email: h.schellekens@ucc.ie; cristina.torres@urv.cat

feedback loop formed by *Bmal1* (brain and muscle aryl hydrocarbon receptor nuclear translocator-like 1) and *Clock* (circadian locomotor output cycles kaput), whose heterodimerization activates the transcription of period (*Per*) and cryptochrome (*Cry*) genes. In turn, PER and CRY results in a feedback inhibition of BMAL1/CLOCK activity<sup>18,19</sup>. Moreover, *Bmal1* can be inhibited by the nuclear receptors REV-ERBa and  $\beta$  (nuclear receptor subfamily 1 group D member 1  $\alpha$  and  $\beta$ ) and activated by RAR-orphan receptor  $\alpha$  and  $\gamma$  (ROR $\alpha$  and  $-\gamma$ )<sup>19</sup>. The central clock synchronizes the different peripheral clocks by neuronal mechanism and hormonal cues, and at this point, the cortisol hormone (corticosterone in rodents) could be one of the potential mechanisms mediating the biological rhythms effects on metabolism.

Cortisol has been suggested as a secondary messenger between central and peripheral clocks, being crucial for the synchronization of host circadian rhythmicity<sup>20,21</sup>, and also essential for the maintenance of metabolic homeostasis, being their alteration involved in metabolic-related disorders development such as obesity<sup>22</sup>. Indeed, high corticosterone/cortisol levels are linked to a variety of diseases, including obesity, dyslipidemia, fatty liver and glucose intolerance<sup>23,24</sup>. An excess of cortisol levels have been associated with an increase in circulating free fatty acids and with adipocyte differentiation in adipose tissue, leading to increased adiposity and insulin resistance<sup>25,26</sup>. Seasonal rhythms have also been shown to influence corticosterone production through the hypothalamus-pituitary-adrenal axis (HPA), which is one of the most important components of the gut-brain axis<sup>27,28</sup>. However, the specific mechanisms underlying the interaction of seasonal rhythms and corticosterone are not yet well elucidated. In this context, gut bacteria may play a key role. Recent studies have shown that glucocorticoids regulate some physiological effects through the gut microbiota<sup>29–31</sup>. In addition, recent evidences link biological rhythms to the gut microbiota composition<sup>32–35</sup>. In fact, aberrant microbiota diurnal fluctuations and dysbiosis caused by external factors such as high fat diet or antibiotic intake, have been associated with altered clock genes expression in the colon and with obesity development<sup>6</sup>. Additionally, our group has recently reported that gut bacteria change depending on photoperiod exposure and that these changes correlate with obesity development in a photoperiod-dependent manner<sup>32</sup>.

Taken together, we hypothesize that gut microbiota may influence corticosterone levels depending on photoperiod conditions in obese rats and that this may be correlated with changes in the seasonal and circadian clock gene expressions. To this aim, corticosterone levels were analyzed in cafeteria diet (CAF)-fed Fischer 344 (F344) rats treated with an antibiotic cocktail (ABX) and housed under different photoperiod conditions to emulate the hours of winter season (short photoperiod, L6), spring/autumn season (standard photoperiod, L12) and summer season (long photoperiod, L18). Standard chow diet (STD)-fed rats and CAF-fed rats without ABX were included as controls. Seasonal and circadian clock gene expression were also analyzed in pituitary gland and colon tissue, which are closely related to the seasonal pacemaker and gut microbiota respectively.

## Results

### Photoperiodic prolife of obese ABX-treated F344 rats

In this study we evaluated if the effects of photoperiods on corticosterone levels are influenced by gut microbiota and associated with changes in the expression of seasonal and clock genes in an obesogenic context induced by CAF.

Data regarding obesity development in STD- and CAF-fed rats are reported in our previous study which goal was to evaluate the effects of photoperiods in obesity development and gut microbiota composition in these animals<sup>32</sup>. In the present analysis, we also included CAF-fed rats treated with ABX to further evaluate the role of gut microbiota in photoperiods-mediated effects. Firstly, body weight (BW) gain was evaluated to confirm that the ABX treatment did not affect CAF-induced obesity rats. No effect of ABX treatment was observed in BW gain under any photoperiod condition ( $p > 0.05$ ) (Figure S1a). Moreover, CAF-fed rats showed decreased glucose tolerance compared to STD-fed rats independently of photoperiod conditions, and this was not affected by ABX treatment (Figure S1b). Finally, ABX did not affect the total caloric intake of CAF-fed animals (Figure S1c).

Regarding photoperiod effects on these parameters, CAF-fed rats housed under L18 conditions exhibited higher BW gain compared with CAF-fed rats housed under L6 conditions ( $p = 0.018$ ) (Figure S1d), but this effect could not be associated to a higher intake in the L18 conditions as significant differences were not shown in the total intake by photoperiod ( $p > 0.05$ ) (Figure S1c). Interestingly, glucose tolerance was higher in CAF-fed rats housed under L18 conditions compared to those housed under L6 ( $p = 0.048$ ) (Figure S1). Moreover, CAF-fed rats treated with ABX showed an interesting photoperiod effect on glucose tolerance, being higher in CAF + ABX rats under L18 condition compared to L6 conditions ( $p = 0.039$ ) (Figure S1e).

Regarding microbiota composition analysis, we previously observed that exposure to L18 conditions significantly altered gut microbiota composition in obese rats<sup>32</sup>. Thus, in the current study, CAF-fed rats were administered with ABX in drinking water (CAF + ABX rats) in order to further disrupt gut microbiota composition. Indeed, ABX significantly altered fecal microbiota composition in these rats (Fig. 1). In this context, ABX treatment strongly reduced fecal microbiota diversity compared to CAF-fed rats independently of photoperiod as revealed by OTUs observed, ACE and Fisher index (Fig. 1a–c). Moreover, the analysis of the overall fecal microbiota composition, visualized by NMDS (non-metric multidimensional scaling), showed that CAF + ABX rats clustered separately from both STD- and CAF-fed rats (Fig. 1d). The relative abundance of several bacteria at phylum and genus levels were also altered by ABX. Thus, ABX treatment led to an overall significant increase of *Proteobacteria* and *Firmicutes* levels (Fig. 1e). At genera level, ABX treatment significantly increased several genera belonging to *Proteobacteria* phylum such as *Sutterrella*, *Citrobacter*, *Enterobacter*, *Erwinia*, *Escherichia*, *Klebsiella* and *Morganella*, and others belonging to *Bacteroidetes* phyla such as *Parabacteroides* and *Prevotella*. Moreover, ABX treatment decreased bacteria genera belonging to *Firmicutes* such as *Lactococcus*, *Streptococcus*, *Clostridium*, and *Coprococcus* (Fig. 1f). Interestingly, the gut microbiota composition of CAF-fed rats was differently affected by ABX depending on photoperiod condition. Most of photoperiod effects were

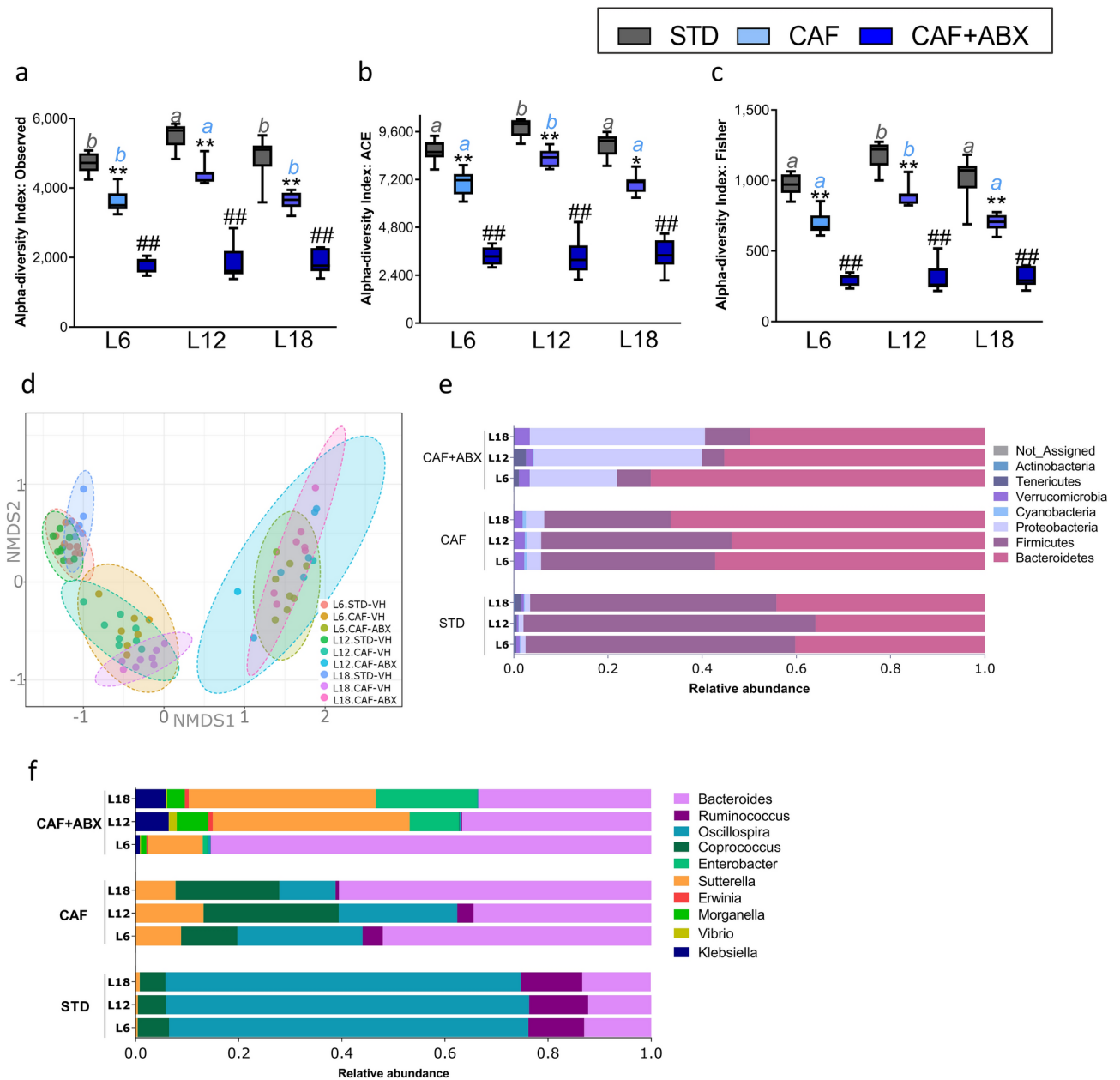


**Fig. 1.** CAF, ABX and photoperiod effects on fecal microbiota composition. (a–c)  $\alpha$ -diversity index calculate by observed operational taxonomic unit (a); abundance-based coverage estimators (ACE) (b); and Fisher (c); \* and # indicate diet and ABX effect respectively analyzed by U-Mann Whitney test (\* $p < 0.05$ ; \*\* $p \leq 0.01$ ; \*\*\* $p \leq 0.001$ ; ## $p \leq 0.001$ ); ab letters indicate photoperiod effect, analyzed by Kruskal–Wallis test followed by Bonferroni correction for multiple comparisons ( $p < 0.016$ ) (d);  $\beta$ -diversity based on Bray–Curtis distances and visualized by a non-metric multidimensional scaling (NMDS)2D plot (PERMANOVA,  $p < 0.001$ ); (e): Stacked bar plots showing the relative abundance of each taxa at phylum level; (f) Stacked bar plots showing the relative abundance of each taxa at genera level. Adapted from Arreaza-Gil *et al.*<sup>32</sup>.

observed in bacteria genera belonging to *Proteobacteria* phyla. Thus, *Sutterella*, *Enterobacter*, *Klebsiella* and *Erwinia* genera were significantly decreased under L6 compared to both L12 and L18 conditions. Moreover, *Bacteroidetes* genera significantly increased under L6 compared to both L12 and L18 (Fig. 1f).

### Corticosterone serum levels were influenced by photoperiod only in ABX-treated rats

Corticosterone serum levels were analyzed in order to elucidate the effects of obesity and ABX treatment in this hormone under different photoperiod conditions. CAF-fed rats showed similar serum levels of corticosterone independently of the photoperiod conditions. When comparing CAF-fed rats with STD-fed rats, significant effects were not found ( $p > 0.05$ ). On the other hand, ABX-treatment did not show any significant effect in corticosterone levels ( $p > 0.05$ ). However, an interesting photoperiod effect was found only in CAF-fed rats

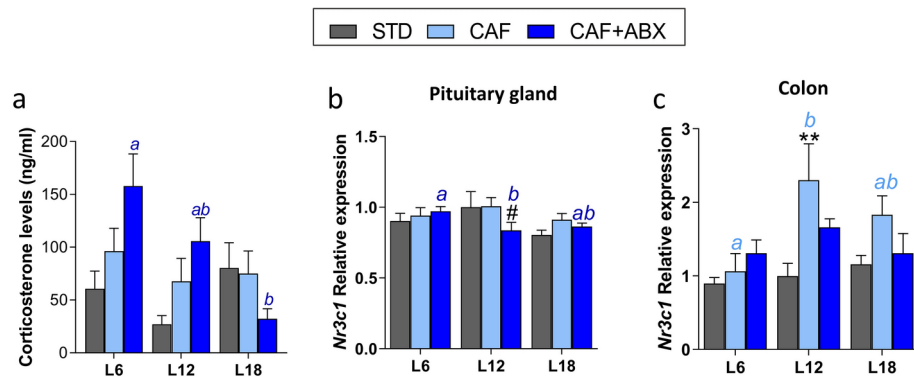


**Fig. 2.** Corticosterone serum levels and GR expression in pituitary gland and colon. (a) Corticosterone serum levels in STD, CAF and CAF treated with ABX rats housed under three different photoperiods (L6, L12 and L18). (b) Relative GR expression (*Nr3c1*) in pituitary gland; (c) Relative gene expression of the GR (*Nr3c1*) in colon tissue; Data were analyzed by two-way ANOVA followed by pairwise comparison Sidak post hoc test: \*indicates CAF effect (\* $p < 0.05$ ; \*\* $p \leq 0.01$ ), #indicates ABX effect (# $p < 0.05$ ) and *ab* letters indicate photoperiod effect in each experimental group; Data are plotted as the mean  $\pm$  SEM ( $n = 7-8$ ). L6: 6 h light/18 h darkness, L12: 12 h light/12 h darkness, L18: 18 h light/6 h darkness, STD: standard chow diet, CAF: cafeteria diet, ABX: antibiotic cocktail (0.5 g/l ampicillin, 0.250 g/l vancomycin and 0.125 g/l imipenem). *Nr3c1*: nuclear receptor subfamily 3, group C, member 1.

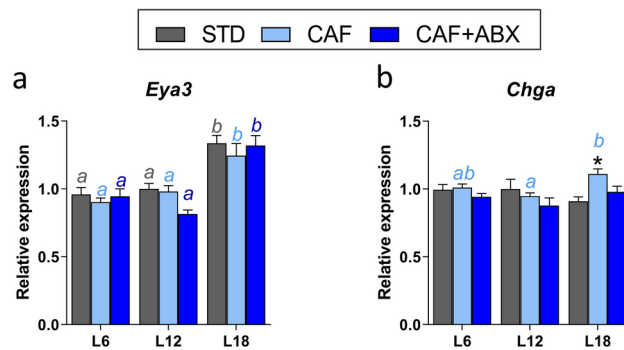


**Fig. 3.** Seasonal genes expression in the pituitary gland. (a) Relative expression of *Eya3* and (b) *Chga* in STD, CAF and CAF treated with ABX rats housed under different photoperiods (L6, L12 and L18). Data were analyzed by two-way ANOVA followed by pairwise comparison Sidak post hoc test: \*\*\* $p \leq 0.001$  and *ab* letters indicate photoperiod effect. Data are plotted as the mean  $\pm$  SEM ( $n = 7-8$ ). L6: 6 h light/18 h darkness, L12: 12 h light/12 h darkness, L18: 18 h light/6 h darkness, STD: standard chow diet, CAF: cafeteria diet, ABX: antibiotic cocktail (0.5 g/l ampicillin, 0.250 g/l vancomycin and 0.125 g/l imipenem).

treated with ABX, being serum corticosterone levels significantly higher in rats housed under L6 compared to those housed under L18 conditions ( $p = 0.009$ ) (Fig. 2a).

Moreover, the gene expression of the glucocorticoids receptor (GR), also known as nuclear receptor subfamily 3, group C, member 1 (*Nr3c1*), was analyzed in pituitary gland and colon tissue. In the pituitary, CAF feeding did not have any significant effect in *Nr3c1* gene expression ( $p > 0.05$ ) (Fig. 2b). However, ABX-treated rats showed significant decreased expression of *Nr3c1* compared to CAF rats only when housed under L12 ( $p = 0.04$ ) (Fig. 2b). Additionally, CAF-fed rats treated with ABX housed under L12 conditions showed decreased expression of this GR compared to those exposed to L6 conditions ( $p = 0.049$ ) (Fig. 2b). Interestingly, the effects observed in *Nr3c1* expression in colon were different to those found in the pituitary gland (Fig. 2c). Colonic *Nr3c1* gene expression increased only in CAF-fed rats housed under L12 conditions ( $p = 0.01$ ) (Fig. 2c). Furthermore, CAF-fed rats showed lower expression of GR under L6 compared to rats housed under L12 conditions ( $p = 0.017$ ).

### ABX treatment in obesity altered seasonal clock in pituitary gland in a photoperiod-dependent manner

The effects of obesity and ABX administration in the relative expression of *Eya3* and *Chga* in the pituitary gland under different photoperiod conditions were also evaluated. The relative expression of *Eya3* was not affected by CAF feeding ( $p > 0.05$ ) (Fig. 3a). However, CAF-fed rats showed increased *Chga* relative expression compared to STD-fed rats only under L18 ( $p = 0.032$ ), resulting in a photoperiod and diet interaction ( $p = 0.017$ ) (Fig. 3b).

Regarding photoperiod effects, the relative expression of *Eya3* was significantly higher in rats housed under L18 conditions, independently of the diet or ABX treatment (L6-STD vs L18-STD,  $p=0.001$ ; L6-CAF vs L18-CAF,  $p=0.004$ ; L6-CAF+ABX vs L18-CAF+ABX,  $p=0.001$ ; L12-STD vs L18-STD,  $p=0.05$ ; L12-CAF vs L18-CAF,  $p=0.04$ ; L12-CAF+ABX vs L18-CAF+ABX,  $p=0.000$ ) (Fig. 3a). In the case of *Chga*, its relative expression was affected by photoperiod in CAF-fed rats, being the expression higher under L18 conditions compared to L12 ( $p=0.048$ ). (Fig. 3b).

### Clock genes expression in pituitary gland and colon was differently affected by photoperiods but not by ABX treatment

Finally, the effects of obesity and ABX treatment in peripheral clock genes expression under different photoperiod conditions were also evaluated. In particular, these were analyzed in the pituitary gland and in colon tissue, two important peripheral clocks in this study due to their relationship with the seasonal pacemaker and the gut microbiota, respectively. In the pituitary gland, obese rats showed increased relative expression of *Bmal1* ( $p=0.001$ ) when housed under L18 conditions (Fig. 4). Moreover, relative clock genes expression in colon tissue were also affected by obesity (Fig. 5). Thus, obesity condition significantly increased the relative expression of *Bmal1* under L12 ( $p=0.016$ ) and L18 conditions ( $p=0.001$ ), and significantly decreased *Per1* expression under L12 condition ( $p=0.047$ ). However, no significant ABX effect was observed in neither the pituitary gland nor in colon ( $p>0.05$ ) (Figs. 4, 5).

Additionally, a photoperiod effect was found in clock genes expression in both pituitary gland and colon tissue. In the pituitary gland, *Bmal1*, *Cry1* and *Rev-erba* showed significant changes in their expression in STD, CAF and CAF+ABX rats depending on the photoperiod conditions, while *Clock* and *Rora* did not show any photoperiod effect ( $p>0.05$ ). In particular, *Bmal1* and *Cry1* expression was significantly higher under L18 independently of obesity and ABX treatment (*Bmal1*: L6-STD vs L18-STD,  $p=0.029$ ; L6-CAF vs L18-CAF,  $p=0.000$ ; L12-CAF vs L18-CAF,  $p=0.000$ ; L6-CAF+ABX vs L18-CAF+ABX,  $p=0.000$ ; L12-CAF+ABX vs L18-CAF+ABX,  $p=0.003$ ; *Cry1*: L6-STD vs L18-STD,  $p=0.001$ ; L6-STD vs L12-STD,  $p=0.000$ ; L6-CAF vs L18-CAF,  $p=0.001$ ; L12-CAF vs L18-CAF,  $p=0.001$ ; L6-CAF+ABX vs L18-CAF+ABX,  $p=0.004$ ; L12-CAF+ABX vs L18-CAF+ABX,  $p=0.005$ ), while *Rev-erba* showed a lower expression under L18 conditions (L6-STD vs L18-STD,  $p=0.000$ ; L6-CAF vs L18-CAF,  $p=0.000$ ; L12-CAF vs L18-CAF,  $p=0.001$ ; L6-CAF+ABX vs L18-CAF+ABX,  $p=0.008$ ) and *Per1* a higher expression under L6 (L6-STD vs L18-STD,  $p=0.019$ ; L6-CAF+ABX vs L12-CAF+ABX,  $p=0.049$ ; L6-CAF+ABX vs L18-CAF+ABX,  $p=0.049$ ) (Fig. 4). In contrast, in colon tissue only *Cry1* and *Rev-erba* showed a significant photoperiod effect independently of the experimental group, (*Cry1*: L6-STD vs L18-STD,  $p=0.004$ ; L12-STD vs L18-STD,  $p=0.05$ ; L6-CAF vs L18-CAF,  $p=0.002$ ; L6-CAF+ABX vs L18-CAF+ABX,  $p=0.05$ ; *Rev-erba*: L6-STD vs L18-STD,  $p=0.005$ ; L12-STD vs L18-STD,  $p=0.000$ ; L6-CAF vs L18-CAF,  $p=0.017$ ; L6-CAF+ABX vs L18-CAF+ABX,  $p=0.000$ ; L6-CAF+ABX vs L12-CAF+ABX,  $p=0.05$ ), *Bmal1* expression showed a photoperiod effect only in CAF-fed rats with and without ABX treatment, being significantly lower under L6 (L6-CAF vs L18-CAF,  $p=0.003$ ; L6-CAF+ABX vs L18-CAF+ABX,  $p=0.041$ ; L6-CAF+ABX vs L12-CAF+ABX,  $p=0.036$ ). *Clock*, *Per1* and *Rora* did not show a significant photoperiod effect ( $p>0.05$ ) (Fig. 5).

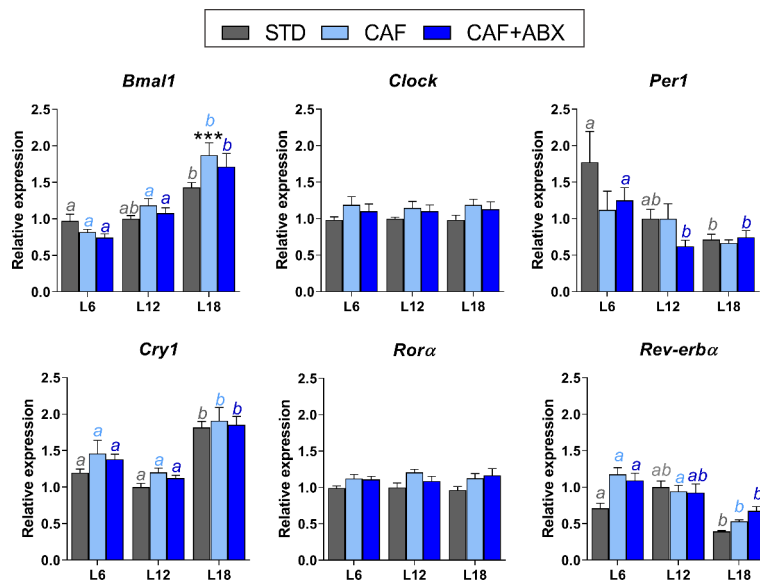


**Fig. 4.** Clock genes expression in pituitary gland. Data were analyzed by two-way ANOVA followed by pairwise comparison Sidak post hoc test: \*indicates diet effect ( $***p \leq 0.05$ ), and *ab* letters indicate photoperiod effect in each photoperiod effect. Data are plotted as the mean  $\pm$  SEM ( $n=7-8$ ). L6: 6 h light/18 h darkness, L12: 12 h light/12 h darkness, L18: 18 h light/6 h darkness, STD: standard chow diet; CAF: cafeteria diet, ABX: antibiotic cocktail.

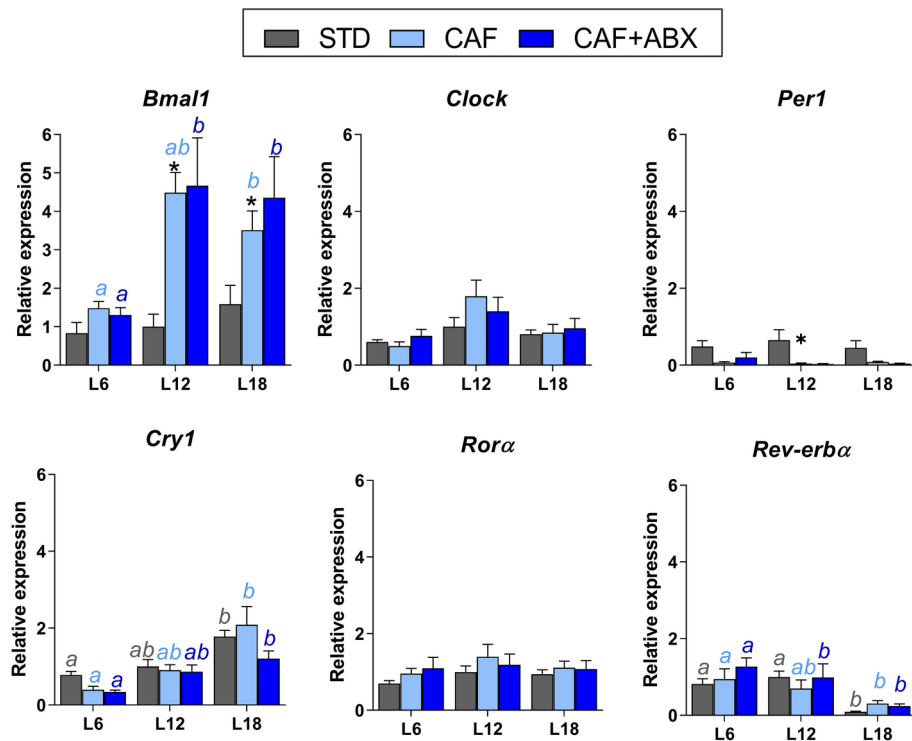


**Fig. 5.** Clock genes expression in colon. Data were analyzed by two-way ANOVA followed by pairwise comparison Sidak post hoc test; \*indicates diet effect (\* $p < 0.05$ ), and *ab* letters indicate photoperiod effect in each experimental group; Data are plotted as the mean  $\pm$  SEM ( $n = 7-8$ ). L6: 6 h light/18 h darkness; L12: 12 h light/12 h darkness; L18: 18 h light/6 h darkness, STD: standard chow diet, CAF: cafeteria diet, ABX: antibiotic cocktail.

## Discussion

Seasonal rhythms have been reported to significantly influence the development of metabolic disorders such as obesity. In this regard, gut microbiota is emerging as a key player in mediating this link between rhythms and obesity, but specific mechanisms are not well understood yet. Corticosterone can be a potential player as it has been described to be affected by both gut microbiota and seasonal rhythms. Thus, studies with germ-free mice have shown that these animals have increased corticosterone response to stress<sup>36</sup> and increased plasma corticosterone levels<sup>37</sup>. Moreover, corticosterone levels have been shown to be influenced by photoperiod conditions, showing lower basal levels in long photoperiod compared to short photoperiod conditions in studies carried out in healthy mice<sup>38</sup>, F344 rats fed a low caloric diet<sup>39</sup> and goats<sup>28</sup>. On the other hand, corticosterone has been linked to the development of metabolic diseases such as obesity<sup>40</sup>. Therefore, this hormone may be crucial in the connection between gut microbiota and biological rhythms effects under an obesogenic context.

In this study, CAF-fed rats did not show any photoperiod effect in corticosterone levels, indicating that the seasonal rhythmicity of this hormone is altered in obesity conditions. Indeed, obesity has been reported to disrupt biological rhythms<sup>5</sup>. Thus, disruption in the diurnal oscillation of corticosterone/cortisol has been reported in animal models of obesity<sup>41</sup> and in obese women<sup>42</sup>, adolescents<sup>43</sup> and children<sup>44</sup>. Moreover, corticosterone levels in CAF-fed rats treated with ABX showed a completely different pattern depending on the photoperiod conditions. Thus, while the dysbiosis of gut microbiota caused by ABX treatment led to increase corticosterone levels in CAF-fed rats housed under L6 and L12 conditions, the levels of this hormone were reduced under L18 conditions, suggesting that gut bacteria influence serum corticosterone levels in a photoperiod-dependent manner. These results correlated with reduced glucose levels in ABX-treated CAF-induced obese rats under L18. In line with this, germ-free animals have also shown alterations in the diurnal corticosterone rhythmicity in intestine, being higher during the active phase, which was linked to the development of hyperglycemia, insulin resistance, and increased triglycerides and free fatty acids<sup>45</sup>. Regarding specific associations between gut microbiota changes and corticosterone levels linked to photoperiods, there were not clear correlations. Hence, as mentioned in the results section, the main photoperiod effects on gut microbiota in ABX-treated rats were observed in bacteria belonging to the *Proteobacteria* phylum. In particular, these bacteria were less abundant in L6 conditions. This is interesting as *Proteobacteria* have been linked to higher cortisol levels in humans<sup>46</sup> and higher corticosterone levels in animal<sup>47</sup> studies. However, in this study this correlation was not observed, as ABX-treated rats housed under L6 conditions showed a reduction in *Proteobacteria* and higher corticosterone levels compared to rats housed under other photoperiod conditions. Therefore, further studies are needed in order to identify specific bacteria involved in corticosterone homeostasis.

On the other hand, the effect of gut microbiota on biological rhythms-mediated oscillations in serum and intestinal corticosterone could be mediated by the modulation of the molecular clock in central and peripheral tissues. In fact, in the above mentioned study, the depletion of gut microbiota also led to the complete disruption of circadian gene expression in ileum which was linked to the effect on corticosterone levels<sup>45</sup>. Thus, the lack of gut microbiota led to increased expression of *ROR $\alpha$*  and *Rev-erba* clock genes, which in turn activated the expression of *Cyp11a1*, the enzyme that catalyzes the first step in the conversion of cholesterol into steroid hormone. This event results in an overproduction of corticosterone in the intestine, resulting in metabolic alterations<sup>48</sup>. Therefore, in this study, the effects on the expression of seasonal and circadian clocks genes were also investigated in pituitary and colon tissue to elucidate potential associations with corticosterone levels. In this regard, a clear photoperiod effect was observed for *Eya3* gene expression as expected<sup>12,49</sup>, and it was independent of ABX, indicating that gut microbiota may have limited influence in this effect. However, in the case of *Chga*, the photoperiod effect observed in CAF-fed rats was not observed in ABX-treated rats indicating that gut microbiota may have a higher influence in this seasonal gene. This is of interest as there is very limited literature regarding this seasonal gene and further studies are needed in order to clarify its role in gut microbiota-mediated impact on seasonal rhythms effects in corticosterone levels. Moreover, *Chga* has been reported to be activated under short photoperiod conditions in male sheep<sup>12</sup>, and here this was not observed. Hence further studies are needed to clarify *Chga* oscillations related to photoperiod conditions in mammals. As for clock genes, ABX did not show any effect on their expression in the pituitary or colon, which is consistent with other studies where ABX and germ-free mice did not modify the oscillation and expression of circadian clocks<sup>50,51</sup>.

In addition, corticosterone mediates many of its effects by altering gene transcription through its interaction with its receptor<sup>52</sup>. It is known that peripheral tissues have high GR levels, which influence the expression of circadian rhythm-related genes. Interestingly, a photoperiod effect was observed for GR receptor in the pituitary for ABX-treated CAF-fed rats, which showed higher levels under L6 compared to L12 conditions. Moreover, ABX treatment also decreased GR expression in CAF-fed rats only when housed under L12 conditions. This reinforces a potential role for gut bacteria in corticosterone signaling influenced by photoperiod conditions. In the case of colon tissue, GR expression was significantly affected by photoperiod in CAF-fed rats without ABX, being lower when rats were housed under L6 condition. This could be due to the fact that obesity can decrease intestinal barrier integrity promoting inflammation and increasing the GR expression<sup>53,54</sup>. Moreover, gut microbiota dysbiosis induced by CAF can also contribute to this increased inflammation and GR expression in colon. Thus, as we have previously reported, CAF significantly altered phyla such as *Proteobacteria*, which has been linked to high grade of inflammation and risk of metabolic disorders<sup>55</sup>.

## Conclusion

These results suggest that gut microbiota influence photoperiod effects on corticosterone and colonic GR expression levels as well as on seasonal clock. However, it has little impact on circadian clocks gene expression in the pituitary and in colon tissue in obese rats. This interaction between gut microbiota, seasonal rhythms and corticosterone may be one of the main mechanisms driving seasonal oscillations of several metabolic and physiologic processes involved in obesity development. These results reinforce the importance of biological rhythms and gut microbiota when investigating metabolic-related pathologies. This is a new field in continuous growth which may improve efficacy of current and new therapies for disease prevention and treatment. However, this study has some limitations such as the complex experimental design with several groups that may lead to miss some statistical effects. Hence, further studies are needed to clarify the impact of gut microbiota in circadian and seasonal clocks and to elucidate the potential mechanisms involved.

## Materials and methods

### Experimental procedure

The experimental design used in the current study has been previously described by our group<sup>32</sup> to determine the effect of different photoperiod on obesity. Now, in this study, we further evaluate if photoperiod effects are influenced by the gut microbiota because we included CAF-induced obese rats treated with an ABX and evaluated the different parameters showed in this article to elucidate our hypothesis. Briefly, thirteen weeks-old male F344 rats ( $n=72$ ) from Janvier Laboratories (Le Genest-Saint-Isle, France) were pair-housed at standard conditions (22°C, 65% relative humidity and 12:12 h light/dark cycle) with *ad libitum* access to water and STD for one week. After this week of adaptation to the facilities, rats were weighted and randomized distributed into three different light–dark cycles (photoperiods) conditions for 9 weeks (light density 350 lx): short photoperiod [L6, 6 h light/18 h darkness], standard photoperiod [L12, 12 h light/12 h darkness], or long photoperiod [L18, 18 h light/6 h darkness], mimicking winter, autumn/spring, or summer day lengths respectively. For each photoperiod condition, rats were further randomly divided in three groups ( $n=8$ ): (1) rats fed a STD (72% carbohydrate, 8% lipid, and 19% protein (Safe-A04c); SAFE, Barcelona, Catalonia, Spain), (2) rats fed a CAF (58% CH, 31% lipid, and 11% protein), and (3) CAF-fed rats treated with ABX during the last 4-weeks (Fig. 6). CAF was freshly prepared every day and included the following (grams per rat and per day): biscuits with pâté and cheese (15–17 g), bacon (7–10 g), ensaimada (pastry) (10–15 g), carrot (11–12 g), standard chow (20–25 g) and milk containing 22% sucrose (w/v). The ABX (0.5 g/l ampicillin, 0.250 g/l vancomycin and 0.125 g/l imipenem; Discovery fine chemicals Ltd, Wimborne, Dorset, United Kingdom) was freshly prepared every day and administered in drinking water. BW and intake were recorded weekly during the whole experimental procedure (Figure S1). Intake was measured per cage ( $N=4$  since rats were pair-housed). Oral glucose tolerance test (OGTT) was carried out in the last week of the experiment. Glucose was orally administered after 6 h of fasting (2 g/kg BW, 50% w/v) and blood glucose levels were measured with a glucometer (Glucocard SM;

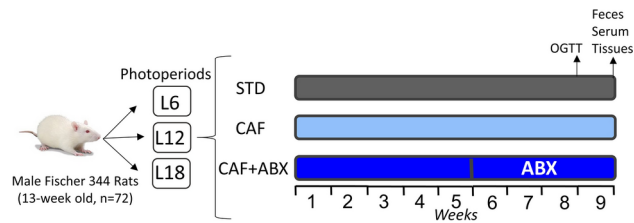


**Fig. 6.** Experimental design. 13-week-old male F344 rats were pair-housed under three different photoperiods (6, 12 or 18 h of light per day) for 9 weeks. In each photoperiod, rats were fed a STD or CAF diet. During the last 4 weeks, a group of CAF-fed rats were treated with an antibiotic cocktail (ABX) in drinking water (ampicillin: 0.5 g/l, vancomycin: 0.25 g/l, imipenem: 0.125 g/l). All rats were sacrificed at the same time point (3 h after the light was turned on, i.e., ZT3). *F344*: fischer 344 rats, *OGTT*: oral glucose tolerance test, *L6*: 6 h light/18 h darkness, *L12*: 12 h light/12 h darkness, *L18*: 18 h light/6 h darkness, *STD*: standard chow diet, *CAF*: cafeteria diet.

Menarini Diagnostics, Barcelona, Catalonia, Spain) at 0, 15, 30, 60 and 120 min after glucose administration (Figure S1).

All animals were sacrificed by decapitation at the same time point, 3 h after the light was turned on, i.e., *zeitgeber* time (ZT3) in order to avoid diurnal rhythmic variations. Pituitary gland and colon tissue were freshly collected and immediately snap-frozen in liquid nitrogen and stored at  $-80^{\circ}\text{C}$  until further analysis. Fecal samples were freshly collected from colon and immediately snap-frozen for 16S rRNA analysis. The blood was collected from the neck, in non-heparinized tubes, incubated for 1 h at room temperature and immediately centrifuged at  $1200\times g$  for 15 min to collect the serum. All experimental protocols were approved by the Animal Ethics Committee of the University Rovira i Virgili (Tarragona, Spain) and the Generalitat de Catalunya (number reference 9495). All methods were carried out in accordance with the guidelines and regulations of the EU Directive 2010/63/EU for animal experiments. Moreover, all methods are reported in accordance with ARRIVE guidelines (<https://arriveguidelines.org>) for the reporting of animal experiments.

### 16S rRNA analysis

16S rRNA analysis was previously described by our group<sup>32</sup>. Briefly, DNA was isolated from fecal samples using QiAmp Fast DNA stool mini kit (Qiagen Inc., Germany). The V3 and V4 regions were amplified using the following primer pairs: 341F-532R (5'-CCTACGGGRSGCAGCAG-3'; 5'-ATTACCGCGGCTGCT-3') and 15F-806R (5'-GTGCCAGCMGCCGCGGTAA-3'; 5'-GGACTACHVGGGTWTCTAAT-3'). The quality, length and concentration of the libraries were analyzed (Bioanalyzer 2100, Agilent). Samples were loaded on a 530 chip (Ion 530TM Chip kit-4 reactions) and sequenced using the Ion S5 system (Life Technology, USA). Among the different conditions evaluated in the current study a total of 63.212.452 sequences were obtained after filtering low-quality reads (phred quality score  $< 17$ ; PGM Software) and analyzed by QIIME (Quantitative insights into microbial ecology) and GreenGenes database. A BIOM format file with the taxa abundance profiles, was obtained and used for the subsequent statistical analysis.

### Corticosterone levels analysis

Serum hormone corticosterone concentration was measured by liquid chromatography coupled to a triple quadrupole mass spectrometer (LC-QqQ). 250  $\mu\text{L}$  of methanol with internal standard (2 ng/mL) was added to 50  $\mu\text{L}$  of serum. This mixture was vortexed and centrifuged for 5 min at  $4^{\circ}\text{C}$  and  $252\times g$ . The supernatant was mixed with 700  $\mu\text{L}$  of 0.1% formic acid in water. The sample was loaded to a SPE system previously conditioned with methanol and 0.1% formic acid in water. The compounds were eluted with 500  $\mu\text{L}$  of methanol using a Zorbax Eclipse C18 (150 $\times$ 2.1 mm) column (Agilent Technologies, Santa Clara, CA, USA). Samples were evaporated in a SpeedVac at  $45^{\circ}\text{C}$  and reconstituted with 50  $\mu\text{L}$  of water:methanol (60:40; v/v) for the analysis.

### RNA isolation and real-time polymerase chain reaction quantification

Total RNA was isolated from colon and pituitary gland samples using Total RNA kit I (Omega Bio-Tek, Inc., Norcross, GA, USA) according to the manufacturer's protocol. RNA quality was determined using a NanoDrop ND2000 spectrophotometer (Thermo Fisher Scientific, Santa Clara, CA, USA). RNA of suitable quality was reverse transcribed using a high-capacity complementary DNA reverse-transcription kit (Thermo Fisher, Madrid, Spain). Quantitative real-time polymerase chain reaction (qPCR) was performed using SYBR Green Master Mix on a CFX96 Real-time PCR detection system-IVD (Bio-Rad Laboratories Inc, Barcelona, Spain). The thermal-cycle program used in all qPCRs was 30 s at  $90^{\circ}\text{C}$ , 40 cycles of 15 s at  $95^{\circ}\text{C}$  and 1 min at  $60^{\circ}\text{C}$ . The different analyzed genes were quantified using peptidylprolyl isomerase A (*Ppia*) as housekeeping gene for normalization. The primers used for each gene were obtained from eufofins Genomics (Wolverhampton, West Midlands, United Kingdom) and are shown in (Table 1). Real-time cycle threshold (Ct) values were recorded, normalized to housekeeping gene expression and transformed to relative gene expression value using the  $2^{-\Delta\Delta\text{Ct}}$  corrected for primer efficiency method<sup>56</sup>.

Target	Forward 5'-3'	Reverse 5' -3'
<i>Eya3</i>	TTTGAGTGCCACAGGACTC	CTGAAGAGGCCAAAGGAGGG
<i>Chga</i>	CAGGAGCTGGAACGTAAGCA	CCATCGCTTGCTCTCCATT
<i>Nr3c1</i>	AGCATTACCACAGCTCACCC	CTGCATACAACACCTCGGGT
<i>Bmal1</i>	GGCGTCGGGACAAAATGAAC	AACTTCCGGGACATCGCATT
<i>Per1</i>	CAGTGAGGAGTCTGCTGAGC	GGAGCCTGAAAGTGCATCCT
<i>Cry1</i>	GGACAAGAATCCCGAGGCTC	CATGATGGCGTCAATCCACG
<i>Clock</i>	TCCTTCAGTTCAGCAGCCAG	ATTCCCATGGAGCAACCGAG
<i>Rora</i>	GTGCGTGTCTTGCAATTGTT	GAGAGGGCTCACACAGGAAC
<i>Rev-erba</i>	GCGTCTGGGTGCTTCATTTC	CGGGTGCAAAAGTCCCAAAG
<i>Ppia</i>	CTTCGAGCTGTTGCAGACAA	AAGTACCACCCTGGCACATG

**Table 1.** Primer sequences for gene expression analysis. *Eya3*: eyes absent homolog 3, *Chga*: chromogranin A, *Nr3c1*: nuclear receptor subfamily 3 group C member 1 (glucocorticoid receptor), *Bmal1*: brain and muscle aryl hydrocarbon receptor nuclear translocator like 1, *Per1*: period circadian regulator 1, *Cry1*: cryptochrome 1, *Clock*: circadian locomotor output cycles kaput, *RORα*: orphan nuclear receptor α, *Rev-erba*: nuclear receptor subfamily 1 group D member 1, *Ppia*: peptidylprolin isomerase A.

### Statistical analysis

Data were plotted using Graphpad Prism 8.0 software (Graphpad software Inc, San Diego, CA, USA) showing mean  $\pm$  standard mean error (SEM) of each group. Statistical analysis was performed using SPSS software (IBS SPSS statistics 25, Armonk, NY, USA). Normality as well as homogeneity of variance were tested by Shapiro–Wilk test and Levene test, respectively. BW gain and OGTT over time were analyzed using repeated-measured ANOVA followed by pairwise comparison Sidak post hoc test at each individual time point. For the AUC of BW gain and OGTT, and for the intake, corticosterone levels and gene expression, the differences between groups were assessed by two-way ANOVA followed by pairwise comparison Sidak post hoc test. The two-way ANOVA was performed depending on the factor evaluated: diet and photoperiod factors or ABX and photoperiod factor.

Fecal microbiota analysis were assessed using the MicrobiomeAnalyst web-based tool<sup>57,58</sup>. Briefly,  $\alpha$ -diversity was calculated by either observed operational taxonomic unit (OTUs) index, abundance-based coverage estimators (ACE) index and by Fisher index. Both diet and ABX effects were analyzed by U-Mann Whitney test ( $p < 0.05$ ) and photoperiod effect was analyzed by Kruskal–Wallis test followed by Bonferroni  $P$  correction for multiple comparison ( $p < 0.016$ ).  $\beta$ -diversity was measured based on Bray–Curtis distances and visualized by a Non-Metric Multidimensional Scaling (NMDS) 2D plot. Permutational multivariate analysis of variance (PERMANOVA) was assessed to evaluate the dissimilarity of the fecal microbiota composition among different groups (PERMANOVA,  $p < 0.001$ ). Relative abundance at phylum and genera level were plotted as stacked bar plots and non-parametric U Mann–Whitney/Kruskal–Wallis test was performed to elucidate pairwise differences in the relative abundance of specific bacteria between groups.

The statistical test used for individual analysis, as well as the statistical significances are provided in the figure legends.

### Data availability

All data generated or analyzed and that support the findings of this study are available in this article and its Supplementary Information file. The datasets generated and/or analyzed during the current study are available in the Zenodo repository, <https://doi.org/10.5281/zenodo.12693103>.

Received: 13 April 2024; Accepted: 15 September 2024

Published online: 29 September 2024

### References

- Blüher, M. Obesity: global epidemiology and pathogenesis. *Nat. Rev. Endocrinol.* **15**(15), 288–298 (2019).
- Seifu, C. N., Fahey, P. P., Hailemariam, T. G., Frost, S. A. & Atlantis, E. Dietary patterns associated with obesity outcomes in adults: An umbrella review of systematic reviews. *Pub. Health Nutr.* **24**, 6390–6414 (2021).
- Johnston, J. D., Ordovás, J. M., Scheer, F. A. & Turek, F. W. Circadian rhythms, metabolism, and chrononutrition in rodents and humans. *Adv. Nutr.* **7**, 399–406 (2016).
- Laermans, J. & Depoortere, I. Chronobesity: role of the circadian system in the obesity epidemic. *Obes. Rev.* **17**, 108–125 (2016).
- Kanikowska, D., Sato, M. & Witowski, J. Contribution of daily and seasonal biorhythms to obesity in humans. *Int. J. Biometeorol.* **59**, 377–384 (2015).
- Murakami, M. & Tognini, P. The circadian clock as an essential molecular link between host physiology and microorganisms. *Front. Cell. Infect. Microbiol.* **9**, 1–9 (2020).
- Panda, S. The arrival of circadian medicine. *Nat. Rev. Endocrinol.* **15**, 67–69 (2019).
- Wood, S. & Loudon, A. Clocks for all seasons: Unwinding the roles and mechanisms of circadian and interval timers in the hypothalamus and pituitary. *J. Endocrinol.* **222**, R39–R59 (2014).
- Helm, B. *et al.* Annual rhythms that underlie phenology: biological time-keeping meets environmental change. *Proc. R. Soc. B Biol. Sci.* **280**, 20130016 (2013).
- Dardente, H. *et al.* A molecular switch for photoperiod responsiveness in mammals. *Curr. Biol.* **20**, 2193–2198 (2010).
- Wood, S. H. *The Parts Tuberculosis and Seasonal Timing*. Springer. **10**, 33–54 (2020).

12. Wood, S. H. *et al.* Binary switching of calendar cells in the pituitary defines the phase of the circannual cycle in mammals. *Curr. Biol.* **25**, 2651–2662 (2015).
13. Tackenberg, M. C. & McMahon, D. G. Photoperiodic programming of the SCN and its role in photoperiodic output. *Neural Plast.* **2018**, 8217345 (2018).
14. Johnston, J. D. Measuring seasonal time within the circadian system: Regulation of the suprachiasmatic nuclei by photoperiod. *J. Neuroendocrinol.* **17**, 459–465 (2005).
15. Coomans, C. P., Ramkisoensing, A. & Meijer, J. H. The suprachiasmatic nuclei as a seasonal clock. *Front. Neuroendocrinol.* **37**, 29–42 (2015).
16. Sumová, A., Jáč, M., Sládek, M., Šauman, I. & Illnerová, H. Clock gene daily profiles and their phase relationship in the rat suprachiasmatic nucleus are affected by photoperiod. *J. Biol. Rhythms* **18**, 134–144 (2016).
17. Reppert, S. M. & Weaver, D. R. Coordination of circadian timing in mammals. *Nature* **418**, 935–941 (2002).
18. Young, M. W. & Kay, S. A. Time zones: a comparative genetics of circadian clocks. *Nat. Rev. Genet.* **2**, 702–715 (2001).
19. Takahashi, J. S. Transcriptional architecture of the mammalian circadian clock. *Nat. Rev. Genet.* **183**, 164–179 (2016).
20. Bering, T., Hertz, H. & Rath, M. F. Rhythmic release of corticosterone induces circadian clock gene expression in the cerebellum. *Neuroendocrinology.* **110**, 604–615 (2020).
21. Mavroudis, P. D., Scheff, J. D., Calvano, S. E., Lowry, S. F. & Androulakis, I. P. Entrainment of peripheral clock genes by cortisol. *Physiol. Genom.* **44**, 607 (2012).
22. Kokkinos, A. *et al.* Glucocorticoid metabolism in obesity and following weight loss. *Front. Endocrinol.* **11**, 59 (2020).
23. Dourakis, S. P., Sevastianos, V. A. & Kaliopi, P. Acute severe steatohepatitis related to prednisolone therapy. *Am. J. Gastroenterol.* **97**, 1074–1075 (2002).
24. Samuel, V. T., Petersen, K. F. & Shulman, G. I. Lipid-induced insulin resistance: unravelling the mechanism. *Lancet.* **375**, 2267–2277 (2010).
25. Gathercole, L. L. *et al.* Regulation of lipogenesis by glucocorticoids and insulin in human adipose tissue. *PLoS ONE.* **6**, e26223 (2011).
26. Hauner, H., Schmid, P. & Pfeiffer, E. F. Glucocorticoids and insulin promote the differentiation of human adipocyte precursor cells into fat cells. *J. Clin. Endocrinol. Metab.* **64**, 832–835 (1987).
27. Otsuka, T. *et al.* Photoperiod regulates corticosterone rhythms by altered adrenal sensitivity via melatonin-independent mechanisms in Fischer 344 rats and C57BL/6j Mice. *PLoS ONE.* **7**, e39090 (2012).
28. Alila-Johansson, A., Eriksson, L., Soveri, T. & Laakso, M. L. Serum cortisol levels in goats exhibit seasonal but not daily rhythmicity. *Chronobiol. Int.* **20**, 65–79 (2009).
29. Farzi, A., Fröhlich, E. E. & Holzer, P. Gut microbiota and the neuroendocrine system. *Neurotherapeutics* **15**, 5–22 (2018).
30. Vodička, M. *et al.* Microbiota affects the expression of genes involved in HPA axis regulation and local metabolism of glucocorticoids in chronic psychosocial stress. *Brain Behav. Immun.* **73**, 615–624 (2018).
31. de Weerth, C. Do bacteria shape our development? Crosstalk between intestinal microbiota and HPA axis. *Neurosci. Biobehav. Rev.* **83**, 458–471 (2017).
32. Arreaza-Gil, V. *et al.* Gut seasons: Photoperiod effects on fecal microbiota in healthy and cafeteria-induced obese Fischer 344 rats. *Nutrients* **14**, 722 (2022).
33. Shor, E. K., Brown, S. P. & Freeman, D. A. A novel role for the pineal gland: Regulating seasonal shifts in the gut microbiota of Siberian hamsters. *J. Pineal Res.* **69**, e12696 (2020).
34. Liu, J. *et al.* Seasonal variation influences on intestinal microbiota in rats. *Curr. Microbiol.* **75**, 1006–1010 (2018).
35. Maurice, C. F. *et al.* Marked seasonal variation in the wild mouse gut microbiota. *ISME J.* **9**, 2423–2434 (2015).
36. Luo, Y. *et al.* Translational psychiatry gut microbiota regulates mouse behaviors through glucocorticoid receptor pathway genes in the hippocampus. *Transl. Psychiatr.* **8**, 187 (2018).
37. Neufeld, K. M., Kang, N., Bienenstock, J. & Foster, J. A. Reduced anxiety-like behavior and central neurochemical change in germ-free mice. *Neurogastroenterol. Motil.* **23**, 255–e119 (2011).
38. Oyola, M. G. *et al.* Gut microbiota and metabolic marker alteration following dietary isoflavone-photoperiod interaction. *Endocrinol. Diabetes Metab.* **4**, e00190 (2021).
39. Togo, Y., Otsuka, T., Goto, M., Furuse, M. & Yasuo, S. Photoperiod regulates dietary preferences and energy metabolism in young developing Fischer 344 rats but not in same-age Wistar rats. *Am. J. Physiol. Endocrinol. Metab.* **303**, 777–786 (2012).
40. van Rossum, E. F. C. Obesity and cortisol: New perspectives on an old theme. *Obesity.* **25**, 500–501 (2017).
41. Cano, P. *et al.* Effect of a high-fat diet on 24-h pattern of circulating levels of prolactin, luteinizing hormone, testosterone, corticosterone, thyroid-stimulating hormone and glucose, and pineal melatonin content, in rats. *Endocrine.* **33**, 118–125 (2008).
42. Al-Safi, Z. A. *et al.* Evidence for disruption of normal circadian cortisol rhythm in women with obesity. *Gynecol. Endocrinol.* **34**, 336 (2018).
43. Berdina, O., Madaeva, I., Bolshakova, S., Sholokhov, L. & Rychkova, L. Circadian rhythm of salivary cortisol in obese adolescents with and without apnea: A pilot study. *Front. Pediatr.* **0**, 537 (2022).
44. Yu, T., Zhou, W., Wu, S., Liu, Q. & Li, X. Evidence for disruption of diurnal salivary cortisol rhythm in childhood obesity: Relationships with anthropometry, puberty and physical activity. *BMC Pediatr.* **20**, 1–10 (2020).
45. Mukherji, A., Kobiita, A., Ye, T. & Chambon, P. Homeostasis in intestinal epithelium is orchestrated by the circadian clock and microbiota cues transduced by TLRs. *Cell.* **153**, 812–827 (2013).
46. Aatsinki, A. K. *et al.* Maternal prenatal psychological distress and hair cortisol levels associate with infant fecal microbiota composition at 2.5 months of age. *Psychoneuroendocrinology* **119**, 104754 (2020).
47. Angoa-Pérez, M., Zagorac, B., Francescutti, D. M., Theis, K. R. & Kuhn, D. M. Responses to chronic corticosterone on brain glucocorticoid receptors, adrenal gland, and gut microbiota in mice lacking neuronal serotonin. *Brain Res.* **1751**, 147190 (2021).
48. Henaoui-Mejia, J., Strowig, T. & Flavell, R. A. Microbiota keep the intestinal clock ticking. *Cell.* **153**, 741–743 (2013).
49. Masumoto, K. H. *et al.* Acute induction of *eya3* by late-night light stimulation triggers TSH $\beta$  expression in photoperiodism. *Curr. Biol.* **20**, 2199–2206 (2010).
50. Thaiss, C. A. *et al.* Microbiota diurnal rhythmicity programs host transcriptome oscillations. *Cell.* **167**, 1495–1510.e12 (2016).
51. Weger, B. D. *et al.* The mouse microbiome is required for sex-specific diurnal rhythms of gene expression and metabolism. *Cell Metab.* **29**, 362–382.e8 (2019).
52. De Guia, R. M., Rose, A. J. & Herzig, S. Glucocorticoid hormones and energy homeostasis. *Horm. Mol. Biol. Clin. Investig.* **19**, 117–128 (2014).
53. Ayroldi, E., Soma, K. K., Brunner, T., Ahmed, A. & Schmidt, C. Extra-adrenal glucocorticoid synthesis in the intestinal mucosa: Between immune homeostasis and immune escape. *Front. Immunol.* **10**, 1438 (2019).
54. Tang, S. *et al.* Intestinal epithelial glucocorticoid receptor promotes chronic inflammation-associated colorectal cancer. *JCI Insight.* **6**, e151815 (2021).
55. Shin, N. R., Whon, T. W. & Bae, J. W. Proteobacteria: microbial signature of dysbiosis in gut microbiota. *Trends Biotechnol.* **33**, 496–503 (2015).
56. Pfaffl, M. W. A new mathematical model for relative quantification in real-time RT-PCR. *Nucleic Acids Res.* **29**, e45–e45 (2001).
57. Chong, J., Liu, P., Zhou, G. & Xia, J. Using microbiome analyst for comprehensive statistical, functional, and meta-analysis of microbiome data. *Nat. Protoc.* **15**, 799–821 (2020).

58. Dhariwal, A. *et al.* MicrobiomeAnalyst: A web-based tool for comprehensive statistical, visual and meta-analysis of microbiome data. *Nucleic Acids Res.* **45**, W180–W188 (2017).

## Acknowledgements

The authors would like to thank Niurka Dariela Llopiz and Rosa Pastor for their technical assistance.

## Author contributions

V.A.G., I.E.-M., J.R.S.-R., and C.T.-F.: methodology. V.A.-G.: formal analysis, visualization data and writing the original draft. H.S., M.S., B.M., C.T.-F., and A.A.-A.: conceptualization. C.T.-F. and A.A.-A.: writing-review and editing manuscript. M.S., B.M., H.S., C.T.-F., and A.A.-A.: funding and resources acquisition. All authors have read and agreed to the published version of the manuscript.

## Declarations

### Competing interests

This work was supported by MCIN/AEI/<https://doi.org/10.13039/501100011033>/ FEDER “Una manera de hacer Europa” (AGL2016-77105-R), Grant PID2020-113739RB-I00 funded by MCIN/AEI/ <https://doi.org/10.13039/501100011033> and “2021/22 Development of a prototype for the establishment of a dysbiosis (alteration) in the intestinal microbiota”, co-financed by Diputació de Tarragona (2021PGR-DIPTA-URV09). V. Arreaza-Gil was supported by the Martí i Franquès Doctoral Fellowships Programme, Universitat Rovira i Virgili (PMF-PIPF-35); I. Escobar-Martínez was supported by the Youth Employment Initiative from the European Social Fund, Ministry of Science, The State Research Agency and Universitat Rovira i Virgili (PEJ2018-002778-A); J.R. Soliz-Rueda was supported by a predoctoral fellowship (Grant Number: BES-2017-080919) from the Ministerio de Ciencia e Innovación MCIN/AEI/<https://doi.org/10.13039/501100011033> and FSE “El FSE invierte en tu futuro. In addition, H. Schellekens and some of the work conducted by V. Arreaza-Gil was supported by a Science Foundation Ireland research centre grant (SFI/12/RC/2273).

### Additional information

**Supplementary Information** The online version contains supplementary material available at <https://doi.org/10.1038/s41598-024-73289-9>.

**Correspondence** and requests for materials should be addressed to H.S. or C.T.-F.

**Reprints and permissions information** is available at [www.nature.com/reprints](http://www.nature.com/reprints).

**Publisher’s note** Springer Nature remains neutral with regard to jurisdictional claims in published maps and institutional affiliations.

**Open Access** This article is licensed under a Creative Commons Attribution-NonCommercial-NoDerivatives 4.0 International License, which permits any non-commercial use, sharing, distribution and reproduction in any medium or format, as long as you give appropriate credit to the original author(s) and the source, provide a link to the Creative Commons licence, and indicate if you modified the licensed material. You do not have permission under this licence to share adapted material derived from this article or parts of it. The images or other third party material in this article are included in the article’s Creative Commons licence, unless indicated otherwise in a credit line to the material. If material is not included in the article’s Creative Commons licence and your intended use is not permitted by statutory regulation or exceeds the permitted use, you will need to obtain permission directly from the copyright holder. To view a copy of this licence, visit <http://creativecommons.org/licenses/by-nc-nd/4.0/>.

© The Author(s) 2024